

**ADVANCES IN
FOREST FIRE
RESEARCH**

DOMINGOS XAVIER VIEGAS

EDITOR

2014

Numerical simulations of spreading fires in a large-scale calorimeter: the influence of the experimental configuration

Y. Pérez-Ramirez^a, P.A. Santoni^a, J.B. Tramoni^a, W.E. Mell^b

^a CNRS UMR 6134, Campus Grimaldi, BP 52, 20250 Corte, France, perez-ramirez@univ-corse.fr

^b US Forest Service Pacific Northwest Research Station, Pacific Wildland Fire Science Laboratory, 400N, 34th Street, Suite 201 Seattle, WA98103, wemell@fs.fed.us

Abstract

The validation of physical models of fire spread requires comparing simulated results and experimental observation. Fire tests conducted at laboratory scale are appropriate to measure the finest physical mechanisms that cannot be recorded at field scale. However, particular attention must be paid concerning the influence of the experimental configuration on the fire and the way to take them into account for the simulation. Indeed, one must be sure that the main effects due to the experimental device and design are well reproduced by the models before to investigate the validation of such model by comparison with thermodynamics quantities measured. In this paper a methodology is proposed to be able to test a physical model against experiments conducted in a Large Scale Heat Release calorimeter. The hood effects as well as the ignition are investigated with WFDS, a physical model of wildland fire.

Keywords: Calorimetry measurements, 3D numerical simulation, WFDS, fire behaviour

1. Introduction

The use of physically-based wildland fire models for research purposes has increased in this last decade both due to their potential to capture the basic physical processes regardless of the scale (Porterie *et al.*, 2005, Mell *et al.* 2007), and due to the growing improvements offered by computational resources. These models have been assessed at different scales but their validation is still ongoing. Laboratory-scale experiments can provide an important source of data for validating physically-based models at this particular scale. However, laboratory fires are relatively low intensity fires and their behaviour is related to the experimental configuration (e.g. experimental methodologies and design, characteristics of the experimental device, etc.). So, when using laboratory experimental data to validate physically-based models, this aspect should be carefully taken into account in order to avoid misleading conclusions.

Figure 1 depicts the different aspects that must be considered to ideally compare the simulation results provided by a given model with experimental observations done at laboratory scale. Depending on the experimental configuration, the design and device parameters might be different. With regard to the experimental design parameters, we can consider that fuel load and slope are common parameters frequently used by many investigators (Dupuy 1995, Viegas 2004, Tihay 2012). Although the range of variation for these parameters might be different from one author to the other, they can be easily (and implicitly) taken into account by physical models. Another important parameter concerning the experimental design is the ignition pattern. Different ignition types (linear or point) and methods can be found in literature. For linear ignition, Viegas *et al.* (2004) use one or more threads of wool soaked in a mixture of petrol and fuel oil. The threads are located at the edge of the fuel bed and ignited with matches. A linear flame is obtained along the thread in 5s. Santoni *et al.* (2010) spread a line of alcohol (4 to 6 ml) linearly on the fuel with a pipette and use a flame torch to ensure quasi-instantaneous ignition along one edge of the fuel. Although for such ignition patterns the fire will spread similarly under no slope condition, conversely ignition condition might affect the spreading for canyon

configuration for instance. Hence providing a numerical ignition close to the experimental one is of interest for the test of physical models. Some parameters that can also affect the spreading of fire are related to experimental device used. For instance the physical properties of the bench substrate are not thermally negligible (Dupuy, 1995). The thermal conductivity of a metallic bench (Viegas, 2004) for instance is different from an air-entrained concrete plate (Santoni *et al.*, 2010). Thus heat transfer between the fuel bed and the bench must be taken into account. Another parameter that can affect fire spreading is the use of an exhaust system. Santoni *et al.* (2010) used such type of system to investigate the heat release rate (HRR) of spreading fires by collecting the smoke released during fire spread. By measuring the consumption of oxygen it is possible to derive the HRR. In previous works we investigated the HRR, the radiant and convective fraction of energy release by fire under slope and no slope conditions (Tihay *et al.*, 2012). Those results can be used to validate physical models of fire spread. However the exhaust system has to be taken into account in the numerical study since the air entrainment near the fire can slightly be modified by the extraction system for low intensity fires. Finally, besides experimental design and experimental device parameters that must be accounted for, the numerical computational parameters (grid size sensitivity, parallelisation,) are of primarily importance. The size of the mesh must be fine enough to couple with both combustion of gases and heat transfer within the fuel bed.

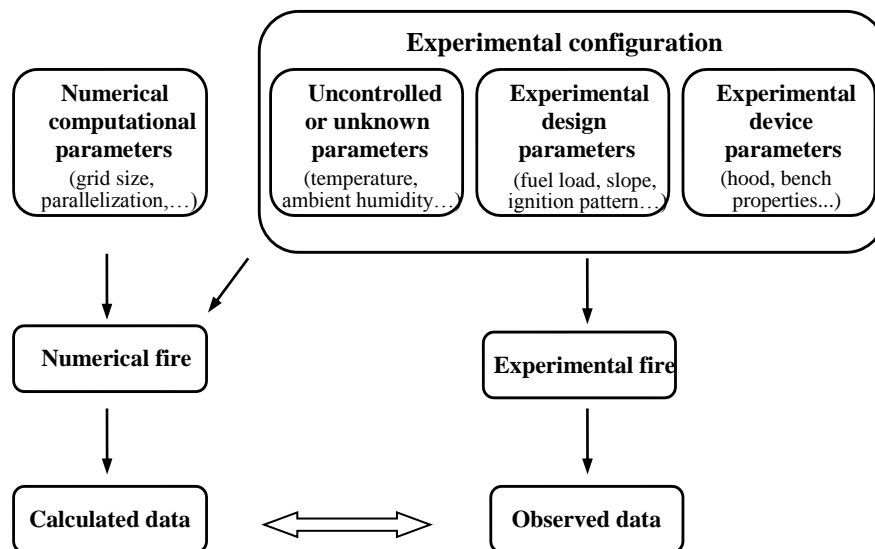


Figure 1. Diagram of the influence of the experimental conditions on numerical and experimental fires

In this paper the use of a physically-based model to simulate spreading fires in a large-scale heat release calorimeter is addressed, paying special attention to the influence of the experimental configuration. The study has been focused on two parameters which could have a major role in the behaviour of numerical fires; this is the hood extraction system and the ignition method. The experimental configuration is first depicted. Then some experimental results are provided to detail the quantities of interest to be modeled. The numerical model is presented in the fourth section. It is the *Wildland urban interface Fire Dynamics Simulator* – WFDS (Mell *et al.*, 2007; Mell *et al.*, 2009) developed by the National Institute of Standards and Technology (NIST) and the US Forest Service. The air flow in the hood is then studied as well as the numerical ignition. A grid sensitivity analysis is performed for the flow to reach a compromise between precision and simulation time.

2. Experimental configuration

The fire spread experiments were conducted by using a 1 MW Large Scale Heat Release rate apparatus (LSHR). Fire tests were performed on a 2 m long and 2 m wide combustion table located under a 3 m × 3 m hood with a 1 m³/s extraction system (Figure 2). Two thermocouples (48 cm spaced) recorded the temperature of the combustion gases in the exhaust smoke duct. The bench was located on a load cell (sampling rate 1 Hz and 1 g accuracy) in order to record the mass loss over time during the fire spread across a fuel bed. Needles of *Pinus pinaster* were distributed uniformly on the table in order to obtain homogenous fuel beds of 1 m width and 2 m long that occupy only the central part of the table. Particular attention was paid to the preparation of the fuel bed. Different fuel loads were tested: 0.6, 0.9 and 1.2 kg/m² that correspond respectively to fuel beds height of 4 cm and 6 cm for the highest loads. At least four repetitions were carried out for each fuel load.

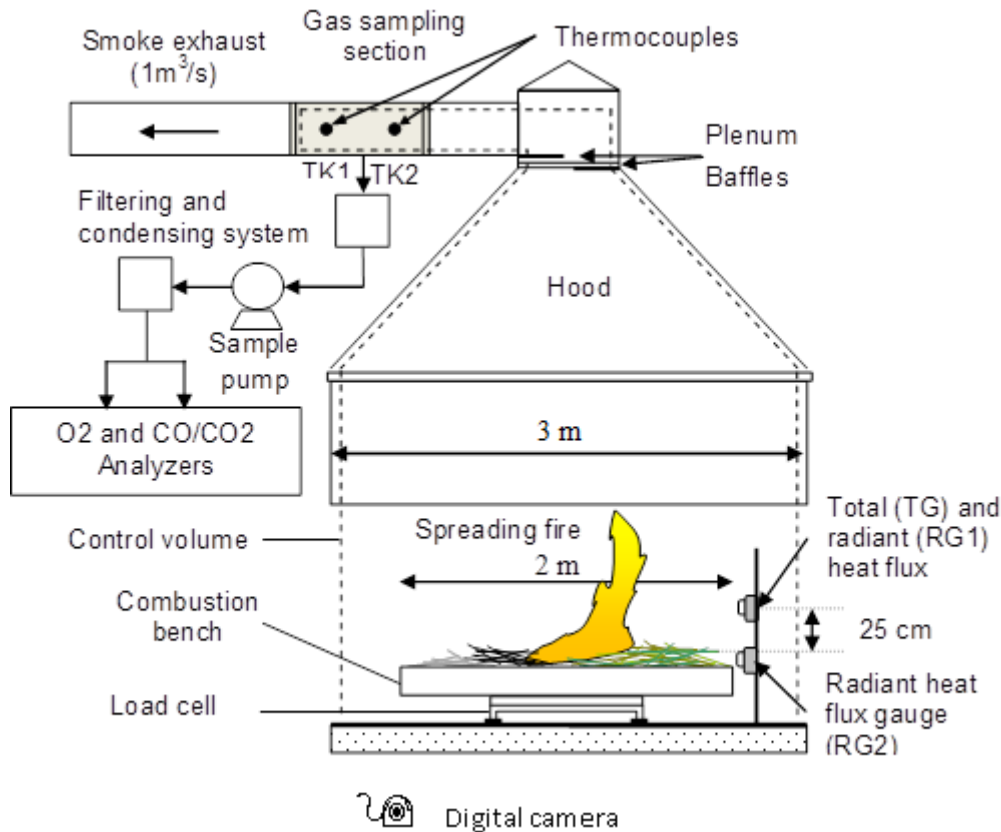


Figure 2. Large Scale Heat Release apparatus used for the fire tests

The net heat of combustion, the surface to volume ratio and density of the particles were $\Delta H_{c,needles} = 20313$ kJ/kg, $\sigma = 3057$ /m and $\rho = 511$ kg/m³ respectively. The net heat of combustion was derived from the gross heat of combustion measured in an oxygen bomb calorimeter following the standard AFNOR NF EN 14918. The needles were oven dried at 60°C for 24 hours. The resulting moisture content was between 3-5%. To ensure fast and linear ignition, a small amount of alcohol and a flame torch were used. The fire tests were conducted without wind under slope angles of 0° and 20°. The rate of spread was deduced from the position of the fire over time every 0.25 m. Three heat flux gauges (Medtherm Corporation) were placed at the end of the experimental bench, in the centre of the bed (see Figure 2 for no slope fire). The total heat flux gauge (TG) and a radiant heat flux gauge (RG1) were oriented towards the flame and located 0.20 m above the bed. The second radiant heat flux gauge (RG2) was located at the end of the combustion bench, at mid height of the fuel layer in order to measure radiation from the bed (Figure 2).

3. HRR measurement and main experimental results

The experiment performed allowed us measuring an important quantity of data: fire front geometry (flame height, flame angle), rate of spread, heat release rate (HRR), burning rate, convective and radiant fraction, radiant heat flux. However for the purpose of this study we solely consider the HRR as it is among the most important parameter for understanding combustion process and fire characteristics (Babrauskas and Peacock, 1992). The measurement of exhaust flow velocity and gas volume fractions were used to determine the heat release rate (HRR) based on the formulation derived by Parker (1992). The heat release rate is given by the oxygen molar flow rate:

$$HRR = E (\dot{n}_{O_2}^{\circ} - \dot{n}_{O_2}) W_{O_2} \quad (1)$$

where $\dot{n}_{O_2}^{\circ}$ and \dot{n}_{O_2} represent respectively the molar flow rates of O_2 in incoming air and in the exhaust duct and W_{O_2} is the molecular weight of oxygen. The volume flow rate of incoming air, referred to standard conditions is:

$$\dot{V}_a = \frac{\dot{n}_{O_2}^{\circ} W_{air}}{X_{O_2}^{\circ} \rho_0} \quad (2)$$

where $X_{O_2}^{\circ}$ is the molar fraction of O_2 in incoming air and W_{air} is the molecular weight of dry air at 25 °C and 1 atm. The oxygen depletion factor is introduced for convenience. It is given by:

$$\phi = \frac{\dot{n}_{O_2}^{\circ} - \dot{n}_{O_2}}{\dot{n}_{O_2}^{\circ}} \quad (3)$$

Combining Eq. (1) - (3), one obtains the HRR, \dot{q} :

$$\dot{q} = \frac{E \rho_0 W_{O_2}}{W_{air}} X_{O_2}^{\circ} \phi \dot{V}_a \quad (4)$$

Gases are measured on a dry basis since the analyzers cannot handle wet mixtures. Thus, the mole fraction of gases in air is derived from the analyzers' measurement and from air humidity. For instance, the mole fraction of oxygen in air is given by:

$$X_{O_2} = (1 - X_{H_2O}) X_{O_2}^a \quad (5)$$

where superscript a denotes the mole fraction in the analyzers. Unfortunately, in an open system, not the incoming air flow rate \dot{V}_a but the flow rate in the exhaust duct \dot{V}_s is measured. A relationship between \dot{V}_a and \dot{V}_s is obtained and after some development (Parker, 1992), the HRR is given by the three following relations:

$$\dot{q} = \frac{E \rho_0 W_{O_2}}{W_{air}} (1 - X_{H_2O}^{\circ}) X_{O_2}^{a^{\circ}} \dot{V}_{s,298} \left[\frac{\phi}{(1 - \phi) + \alpha \cdot \phi} \right] \quad (6)$$

$$\dot{V}_{s,298} = 22.4 A \frac{k_t}{k_p} \sqrt{\frac{\Delta P}{T_s}} \quad (7)$$

$$\phi = \frac{X_{O_2}^{a^\circ}(1 - X_{CO_2}^a) - X_{O_2}^a(1 - X_{CO_2}^{a^\circ})}{X_{O_2}^{a^\circ}(1 - X_{CO_2}^a - X_{O_2}^a)} \quad (8)$$

X denotes the molar fraction and ρ_0 is the density of dry air at 298K and 1 atm. $\dot{V}_{s,298}$ is the standard flow rate in the exhaust duct. α is the expansion factor for the fraction of the air that was depleted of its oxygen. The superscript $^\circ$ is for the incoming air. A is the cross sectional area of the duct, k_t is a constant determined via a propane burner calibration, $k_p=1.108$ for a bi-directional probe, ΔP is the pressure drop across the bi-directional probe and T_s is the gas temperature in the duct.

Instantaneous heat release rates (HRR) measured during the fire tests are displayed in Figure 3 for fuel loads of 0.6, 0.9 and 1.2 kg/m² and no slope. For experiments performed without slope, a quasi-steady state was reached for all fuel loads. The flameout occurred earlier for higher fuel load due to the increase in the rate of spread. The average HRR were computed during the quasi-steady state. The average heat release rates were 41, 87 and 130 kW for the 0.6 to 0.9 and 1.2 kg/m² fuel load, respectively. The greater the fuel load, the greater the heat release rate. The mean values increased by a factor of 2.1 and 3.2 with increasing the fuel load by a factor of 1.5 and 2. The total heat released (THR) was obtained by integration of the HRR curves during the whole experiment. The average total heat released were 22, 33 and 44 MJ for the 0.6, 0.9 and 1.2 kg/m² fuel load, respectively. The total heat released depends also linearly on the load.

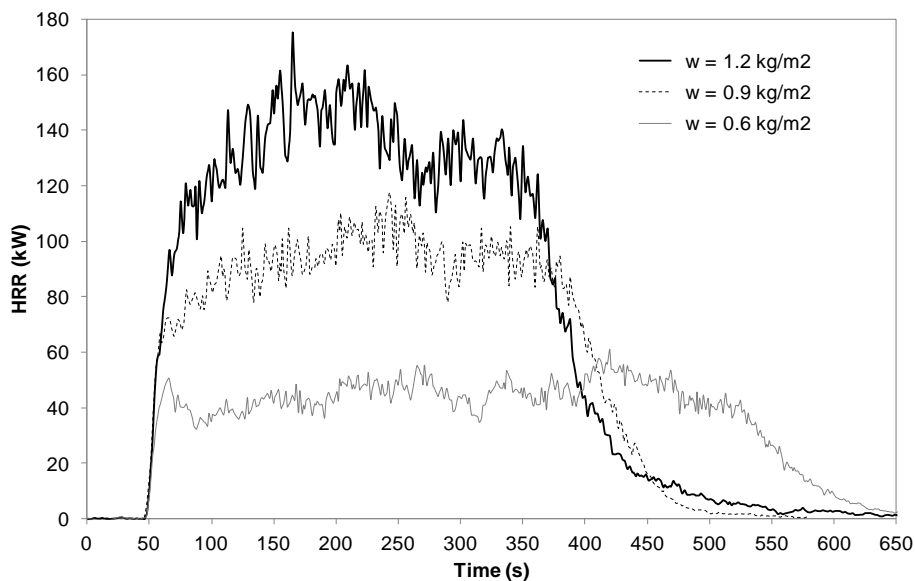


Figure 3 –Heat release rate versus time for fuel load of 0.6, 0.9 and 1.2 kg/m²

4. Numerical model

The numerical approach, called WFDS for WUI Fire Dynamics Simulator, is an extension of the capabilities of the FDS (Fire Dynamics Simulator) to outdoor fire spread and smoke transport problems that include vegetative and structural fuels and complex terrain. FDS is a fire behaviour model developed by NIST in cooperation with VTT Technical Research Center of Finland, industry, and academics (Mc Grattan *et al.*, 2013a). The methods of computational fluid dynamics (CFD) are used to solve the three-dimensional time-dependent equations governing fluid motion, combustion, and heat transfer. The numerical model is based on the large-eddy simulation (LES) approach and provides a time-dependent, coarse-grained numerical solution to the governing transport equations for mass,

momentum, and energy. There are currently two ways of representing vegetative fuel in WFDS. One is restricted to surface fuels (Mell *et al.*, 2007). It is called the boundary fuel model. The other, called the fuel element model can be used for raised or surface fuels but requires more spatial resolution (Mell *et al.*, 2009). The interested reader is referred to Mell *et al.* (2009) for an extended presentation of WFDS and its capabilities. In the present work, we use the fuel element model to represent the vegetation. We assume that the litter is composed of thermally thin fuel elements. The needles of *Pinus Pinaster* are sufficiently small in size (e.g., branches <1.85 mm in diameter) that the heat transfer is not resolved within the core of each needle on the computational grids used here (2 cm). This is similar to other modelling approaches (Porterie *et al.*, 2005). Both convective and radiative heat transfer between the gas phase and the vegetation is accounted for, as is the drag of the vegetation on the airflow. In the modelling approach used here, the temperature equation for the fuel bed is solved assuming a two stage endothermic decomposition process of water evaporation followed by solid fuel pyrolysis. The grid size (2 cm) inside the vegetation litter was evaluated as a fraction of a length scale representative of the radiative heat transfer $\delta_r = 4/(\beta\sigma)$ which constitutes one of the most important modes of heat transfer contributing in many situations to the propagation of the fire. β represents the compactness of the litter. Its value was 0.029 for the fuel loads of 0.6 and 0.9 kg/m² and 0.039 for the fuel load of 1.2 kg/m². The values of δ_r are respectively 4.4 cm for the fuel loads of 0.6 and 0.9 kg/m² and 3.3 cm for the fuel load of 1.2 kg/m². Simulations were run with an Intel Xeon cluster whose nodes consists of two 8-core Intel Xeon E5-2650 CPUs running at 2.0 GHz with 32 GB of main memory.

5. Sensitivity analysis and ignition method

5.1. Sensitivity analysis of the flow in the hood

As detailed previously, calorimetric calculations are based on the measurement of oxygen consumption. A hood extraction system collects the gases released from the combustion, hence this system induces an air flow. Validating a physical model of vegetation requires thus being capable to capture the flow within the hood that could influence the spreading of the fire. In other words, before to test the model against experimental results one must verify previously that it is able to represent the flow without fire, since the flow field could have an influence for fire tests with the smallest fuel load. Indeed, for the load value as 0.6 kg/m², the fire front is not regular and it seems formed of an ensemble of individual flamelet. It is not the case for the highest fuel load (0.9 kg/m² and 1.2 kg/m²) for which the fire front is like a wall of flame spreading towards the unburned fuel. To study the flow we have first considered the whole laboratory of experimentation with the LSHR inside as well as the different vents. Figure 3 depicts the laboratory simulated with WFDS.

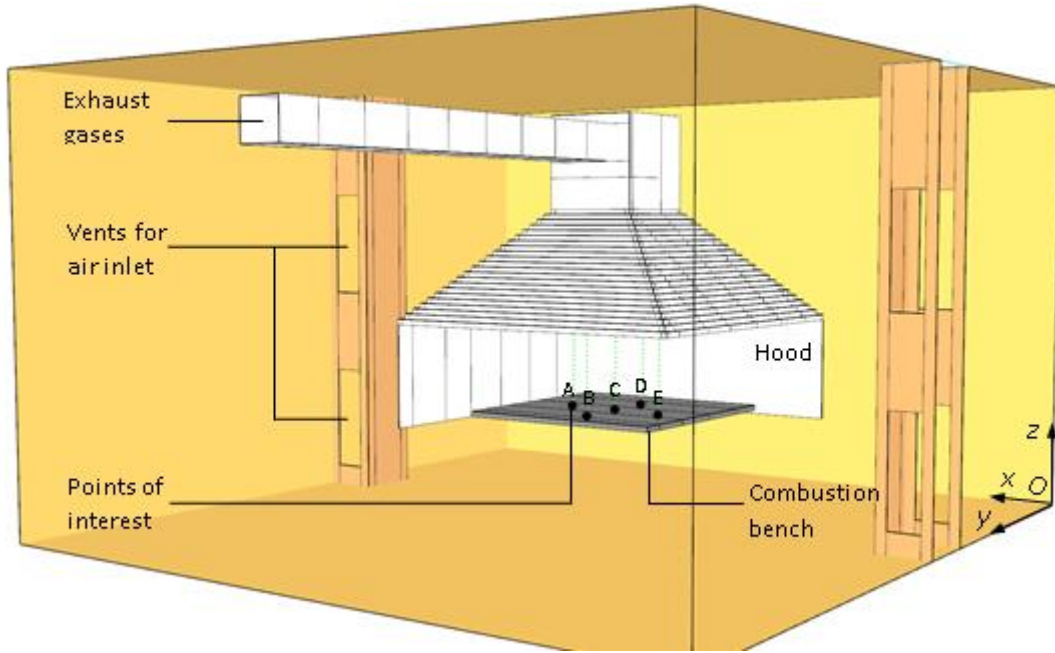


Figure 4. Laboratory with LSHR and vents.

We can see that the domain of calculation is much larger than the LSHR hood where the fire tests were performed. However, before to reduce the size of the calculation domain (to the size of the control volume of the hood as shown in figure 1 for instance) it is important as a first step to conduct a sensitivity analysis with the actual dimension of the experimental laboratory whose dimensions are 6.6 m long, 6.4 m large and 4.4 m high.

Sensitivity analysis

A sensitivity analysis has been performed to find out the more appropriate grid resolution to capture the flow dynamics behavior within the hood. Although the mesh size inside the vegetation is governed by the radiant heat transfer through the fuel bed, conversely a measure of how well the flow field is resolved in the gas phase above the fuel (for simulations involving buoyant plumes) is usually given by the non-dimensional expression $z_c/\delta x$ (Mc Grattan *et al.*, 2013b)

$$z_c = \left(\frac{\dot{q}}{\rho_\infty c_p T_\infty \sqrt{g}} \right)^{2/5} \quad (9)$$

where z_c is a characteristic fire scale, δx is the nominal size of a mesh cell and $\rho_\infty = 1.2 \text{ kg/m}^3$, $c_p = 1000 \text{ J/(kg.K)}$ and $T_\infty = 293 \text{ K}$ are respectively the density, specific heat and temperature of ambient air. The $z_c/\delta x$ values have to range from 4 to 16 (Mc Grattan *et al.*, 2013b). In our case, since the fire is spreading as a line, the characteristic length scale $z_{c,line}$ for a line plume is given by:

$$z_{c,line} = \left(\frac{\dot{q}'}{\rho_\infty c_p T_\infty \sqrt{g}} \right)^{2/3} \quad (10)$$

where \dot{q}' represents the fire line intensity, i.e. the energy release rate per unit length of the fire (Quintiere, 2006). Since the fire front remains quasi-linear during the fire tests, the fire line intensity is equivalent to the HRR: 41, 87 and 130 kW respectively for fuel loads of 0.6, 0.9 and 1.2 kg/m². We obtain $z_{c,line}$ values of 0.11, 0.18 and 0.24 m respectively for the 0.6 to 0.9 and 1.2 kg/m² fuel loads. For these fuel loads, the mesh size δx must respectively be lower than 2.8, 4.6 and 6 cm.

As a first stage, our sensitivity analysis is based on the study of the flow in the hood without the fire. The following mesh sizes were used: 2.5 cm, 5 cm and 10 cm called respectively grid 1, grid 2 and grid 3 in the following. The reason is that away from the fire, the mesh size can be coarse and having mesh size greater than the sizes mentioned previously can provide computational time saving without altering the resolution of the fire region for which the grid has to be finer (less than 2.8, 4.6 and 6 cm for the 0.6 to 0.9 and 1.2 kg/m² fuel loads). For the sensitivity analysis, we will consider 5 positions of interest on the bench on combustion (Figure 4): point C is at the center of the table and points A, B, D and E are positioned 0.5 m aside. The global velocity and the velocity components of the flow will be considered as a function of height above these 5 positions. The interval (Fig 4) between each point along height depends on the mesh size. The total velocity (and deviation) with height are displayed in figure 5 above positions A and C as example. The results presented are representative of simulations obtained at location B, E and F. The better agreement between grid 1 and 2 was obtained at position A while position C is representative of the worst agreement between simulations results obtained with both grids. Figure 5 shows that the values of the total velocity obtained with grid 2 are near to the simulation of reference performed with grid 1. We observe also that grid 3 fails to reproduce the tendency of the variation of the velocity with height observed for grid 1 and 2. The small differences observed between the results obtained with grid 1 and grids 2 suggest that a mesh size of 2.5 cm is sufficient to get convergence in the case of a non reacting flow. Another point that deserves mention is the comparison of inflow at the vent of the domain. The mass balance was checked for the three grids, but we observe that the inflow is very different for grid 3. In that case, a greater amount of air comes into the domain and then flow out at the vent denoting an important recirculation that was very low for grid 1 and grid 2. All these results show that a mesh size of 10 cm is not capable to accurately represent the flow in the hood and in the laboratory.

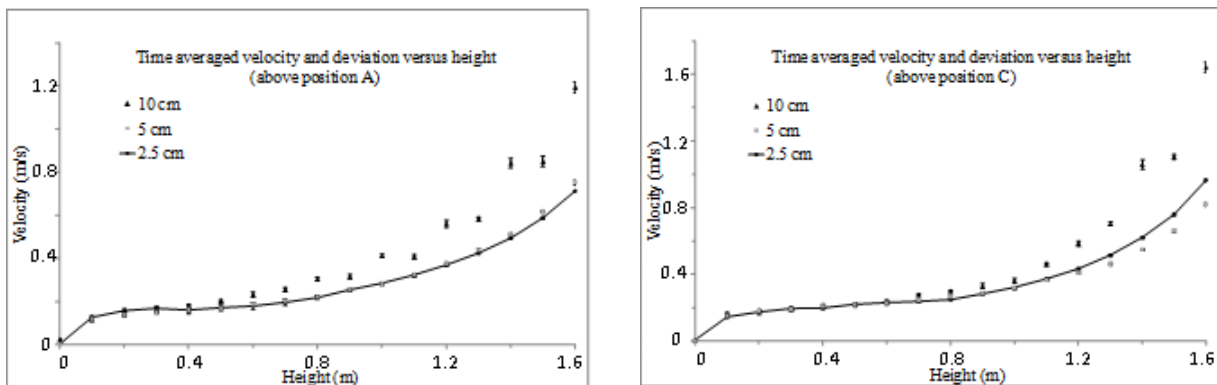


Figure 5. Time averaged velocity and standard deviation versus height in the hood for the large calculation domain (laboratory) above position A and C for the different grids

The quality of a particular simulation is most directly tied to the grid resolution. In order to measure this quality, the fraction of unresolved kinetic energy called the measure of turbulence resolution (MTR) was examined (Mc Grattan *et al.*, 2013b). The MTR is similar to the Pope (2004) criterion. The MTR was calculated at each point above the positions of interests as depicted in figure 4. Then the time average of MTR was calculated at each point along height. And finally the mean of these values was calculated versus height above the five positions of interest. Figure 6 displays the results of the mean time averaged MTR along height for the different grid tested. According to Mc Grattan *et al.* (2013b), maintaining mean values of MTR near 0.2 provides satisfactory results (simulation results within experimental error bounds) for mean velocities and species concentrations in non reacting, buoyant plumes. Hence figure 6 shows that grid 1 and grid 2 are convenient for this criterion while grid 3 is not suitable.

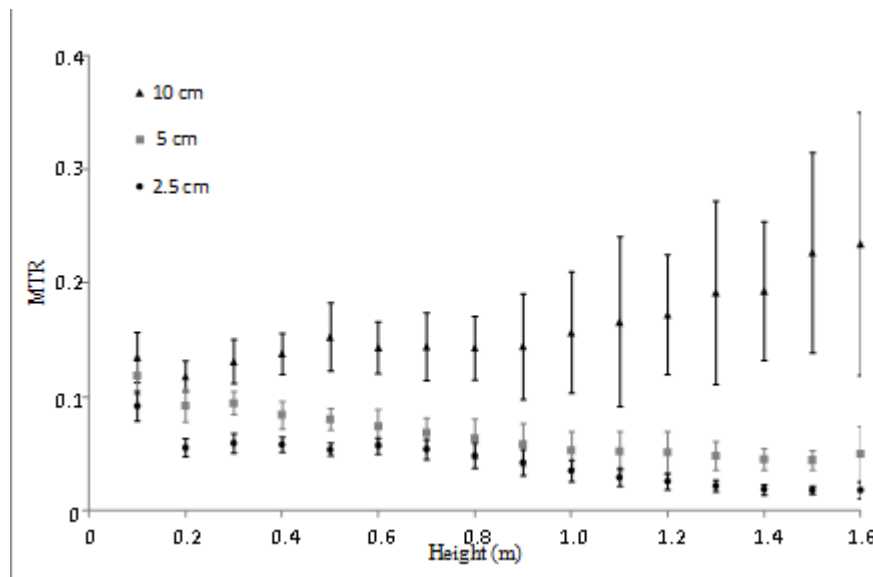


Figure 6. Measure of mean turbulence resolution with standard deviation for the different grids.

Size of the calculation domain and time saving

The size of the calculation domain is an important factor that affect greatly the calculation time. The greater the domain is the larger the time of simulation is. As an example, the simulation time performed per day for the flow is given in table 1 for the mesh sizes of 2.5, 5 and 10 cm (grids 1, 2 and 3). Different domains of calculation have been studied and the simulated results have been compared as previously, attempting to reach a compromise between the precision of the results and the simulation time. Two domains are discussed hereafter. The first one is a little bit larger than the hood (50 cm larger in all direction). It is called 'LSHR and vicinity'. The second one is limited to the size of the hood (see control volume in figure 1). It is called LSHR.

Table 1. Calculation time for the different grids

	Grid 1	Grid 2	Grid 3	Grid 4
Domain	Laboratory	Laboratory	Laboratory	LSHR
Mesh size (cm)	2.5	5	10	2 and 4
Number of mesh	11 489 280	1 436 160	179 520	2 707 200
Number of processor	14	1	1	14
Calculation time (sec/day)	13	29	883	72

In order to optimize the different requirements of the grid (in the litter and in the flame), the mesh size was fixed to 2 cm in the litter, above it and below it (under the bench). A coarse mesh size of 4 cm was used elsewhere in the calculation domain since as seen previously grid 2 (5 cm size) was enough convenient for the flow. We have chosen 4 cm since it is not allowed with FDS to align meshes with size of 2 cm and 5 cm (Mc Grattan *et al.*, 2013a). The simulation of the flow done with these domains was compared to a simulation of reference performed with the large domain (see Figure 2) for which a mesh size of 2 cm was used in the hood and 4 cm elsewhere in the domain to be coherent with the mesh of the small domains.

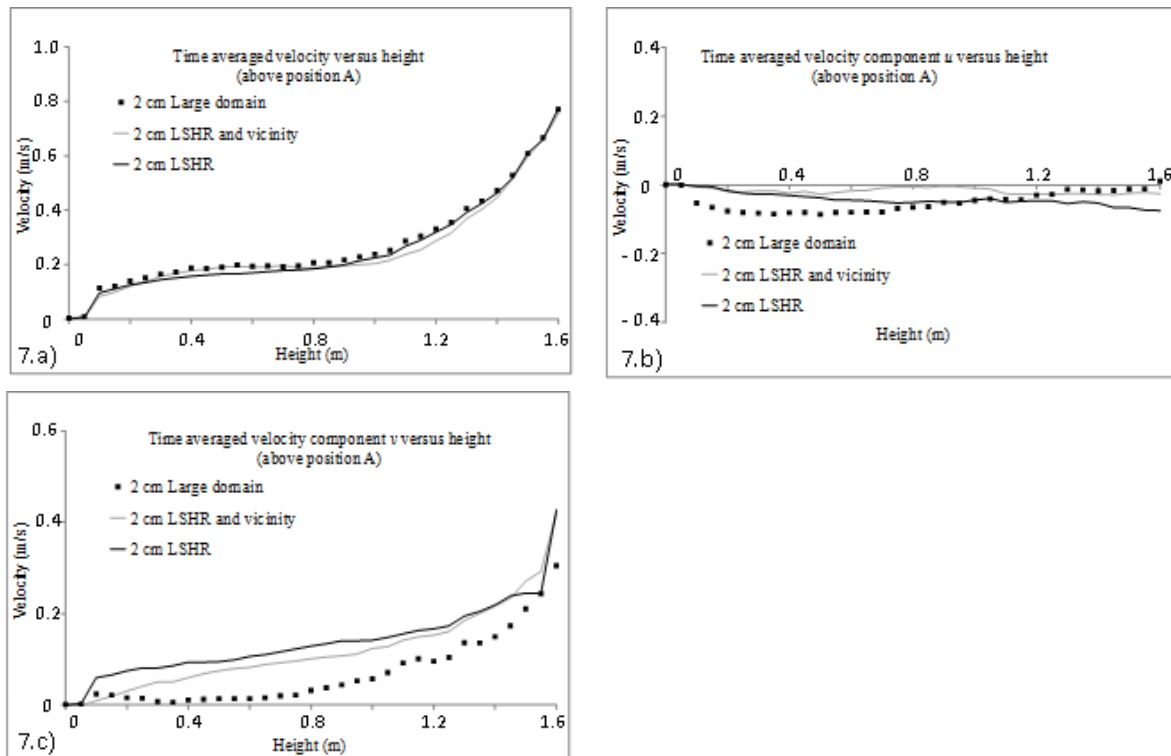


Figure 7. Simulation of the velocity in the hood of the LSHR: comparison between the large calculation domain and the domains limited to the hood and to the hood vicinity: a) global velocity, b) component u , c) component v , d) component w .

Figure 7 shows the time averaged velocity versus height above position A and the time averaged of the three components of the velocity u , v and w along respectively the axis Ox , Oy and Oz as depicted in Fig 2, for the three calculation domain. We observe that for the different positions along the height the three calculation domain provide similar results for the three components of velocity. The LSHR domain is however in better agreement with the large domain than the ‘LSHR with vicinity’ domain for component w . We can note that the values of components u is almost zero along the height and simulation results obtained with both domains can be considered in agreement for u . The main difference between the small domains and the large one is visible for component v which is overestimated with the small domains. However, we can observe that the tendency of components v which increases with height is rendered by the simulation performed with the small domains. Here also, the difference between the results of both small domains is negligible. Similar results were obtained along height for points located above the positions B, C, D and E. We can conclude that both small domains are equivalent to simulate the flow by comparison with the simulations performed with the large domain.

5.2. Ignition method

Concerning the ignition method, experimental fires were ignited by using a small amount of ethanol and a flame torch to ensure a fast and linear ignition of the fuel beds. The fires were ignited along the entire width of the fuel bed by using between 4 and 6 ml of alcohol. Figure 8 displays a zoom of figure 3 to focus on the HRR just at the ignition. 4 ml were used to ignite the fire tests with fuel load of 0.6 kg/m^2 while 6 ml were used to ignite fire tests with higher fuel load.

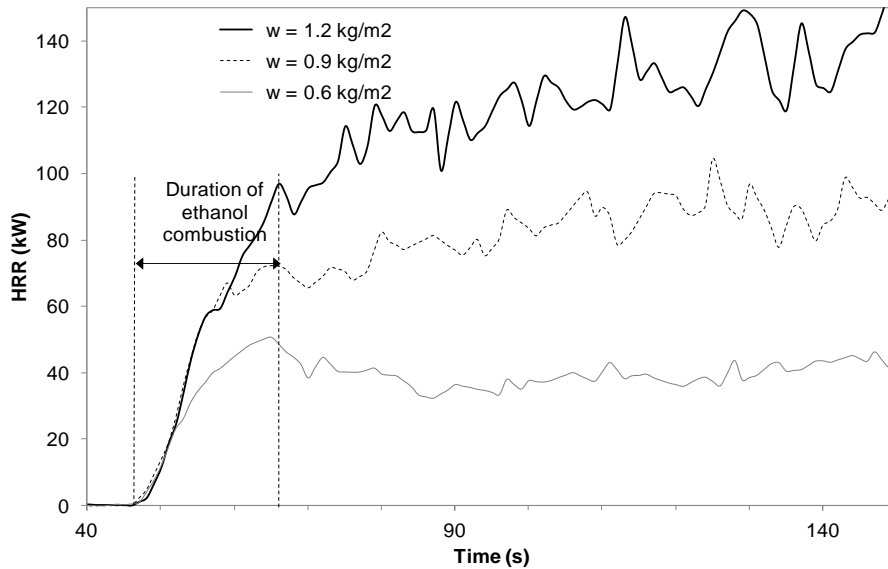


Figure 8 –Heat release rate at the ignition for fuel load of 0.6, 0.9 and 1.2 kg/m²

A study has been performed to investigate the duration time of ethanol burning when it is spread on the combustion bench without the vegetation. We measured this time (see Figure 8) in order to determine the mass of needles burned with ethanol during the ignition, $m_{needles}$:

$$m_{needles} = \frac{\int_0^{t_{ig}} \dot{q} dt - V_{ethanol} \times \Delta H_{c,ethanol}}{\Delta H_{c,needles}}$$

where t_{ig} represents the duration of ignition, $V_{ethanol}$ is the volume of ethanol used to ignite the vegetation and $\Delta H_{c,ethanol} = 21300$ kJ/L is the net heat of combustion of ethanol. The mass of needles involved in the ignition has been estimated to 20 g, 32 g and 35 g respectively for the fuel load of 0.6, 0.9 and 1.2 kg/m². The mass of needles used for 0.9 and 1.2 kg/m² are very close because the same quantity of ethanol was used for both fuel loads.

WFDS offers different options to simulate an ignition source that have been tested to reproduce the experimental ignition. Two different numerical methods to ignite the fuel bed have been compared in order to assess their ability to reproduce our experimental ignition in terms of heat release rate. The first method considers a linear strip of a given width located at the edge of the combustion bench for which the HRR per unit area is fixed during a time interval corresponding to the duration of the ignition. With this method and given the mass of fuel involved in ignition a strip of one meter long and 4 cm wide was considered. Although the calculated width was slightly lower than 4 cm, this dimension was chosen to be in agreement with the mesh size (2 cm) within the fuel bed. The HRR per unit area was set to 1100 kW/m² for the fuel load of 0.9 kg/m². The strip of ignition was applied during 18 s. It should be noted that the fuel bed length was shortened of 4 cm in order to avoid superimposing the needles and the strip that can be viewed as a burner located in front of the fuel bed. The second method consists of fixing the temperature of an ignitor at 1000°C. The ignitor is 4 cm wide and one meter long. Its height is equal to the fuel bed height. The ignitor is like a set of particle with porosity equal to the porosity of the fuel bed. It is located in front of the fuel bed. The simulated results of HRR for both methods of ignition were very similar. A point that deserves mention is the necessary time required “before to ignite the numerical fire”. Even though the time for the flow to reach a quasi-stationary regime is not a problem for experimental fires since the hood is turned on a long time before ignition, it is the case for numerical fires. Indeed, the numerical ignition has to take place once a “quasi-

stationary flow regime” is established. This time is about 60 s for the LSHR domain of calculation and for a fuel load of 0.9 kg/m^2 . Ignition before this time (that is to say during the transient flow regime) might result in a perturbation of the fire line that subsequently affects the spreading of the fire front over time (see Figs. 9a and 9b). In that case, the perturbation of the ignition is due to the flow that is not stabilized and introduces some dissymmetry before a given time that depends on the configuration (height of the fuel bed,...).

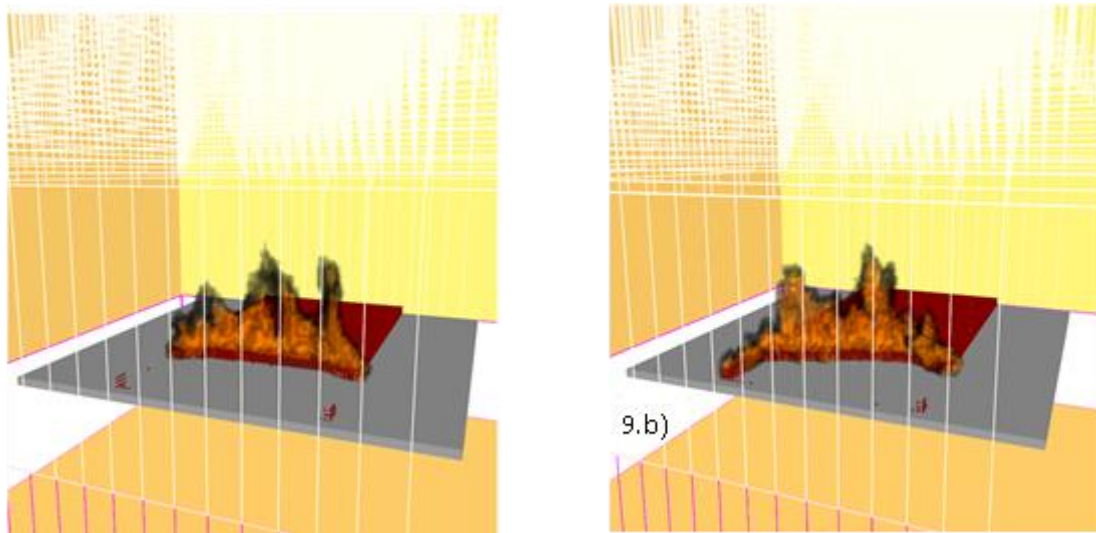


Figure 9. Influence of ignition time on the fire front shape for a fuel load of 0.9 kg/m^2 : a) numerical ignitions performed after stabilisation of the flow, b) numerical ignition performed before stabilisation of the flow

6. Conclusion and prospects

Physical model of fire spread are very promising to represent the behavior of wildland fires at a scale useful for risk assessment and fire safety concerns. The aim of our ongoing study is twofold. We propose a set of experimental data that can be used to validate physical model based on thermodynamics quantity of interest. Secondly we propose a methodology to validate such models paying attention to the influence of the experimental conditions that can affect the comparison between numerical and experimental fires. We focused on two parameters which could have a major role in the behaviour of numerical fires: the hood extraction system and the ignition method. This paper represents the first step of our work. Further studies will be devoted to the following activity: measurements of flow velocity within the hood will be done to assess the accuracy of WFDS to represent the flow with no fire. Secondly a full study will be performed to test WFDS against the set of data obtained from experiments conducted with the calorimeter for fire spreading under both slope and no slope condition for the different fuel loads: HRR, mass burning rate, radiant heat flux and exhaust gas composition. The role of the char during the process of spreading will be particularly investigated.

7. Acknowledgements

Part of this work was carried out in the scope of project PROTERINA-Due supported by the EU under the Axis 3 (Natural and Cultural Resources) of the Operational Program Italia/France Maritime 2007-2013, contract: G25I08000120007.

8. References

- Babrauskas, V., Peacock, R.D. (1992) HRR. The single most important variable in fire hazard. *Fire Safety Journal* **18**, 255-292.
- Dupuy J.L. (1995) Slope and fuel load effects on fire behavior: laboratory experiments in pine needles fuel beds, *International Journal of Wildland Fire*, **5(3)** 153-164
- McGrattan K., Hostikka S., McDermott R., Floyd J., Weinschenk C., Overholt K. (2013a) Fire Dynamics Simulator Technical Reference Guide, volume 1 : Mathematical Model. Technical Report. NIST Special Publication, 1018-6, National Institute of Standards and Technology, Gaithersburg, Maryland, <<http://fire.nist.gov/fds>>.
- McGrattan K., Hostikka S., McDermott R., Floyd J., Weinschenk C., Overholt K. (2013b) Fire Dynamics Simulator User's Guide. Technical Report NIST Special Publication, 1019-6, National Institute of Standards and Technology, Gaithersburg, Maryland, <<http://fire.nist.gov/fds>>.
- Mell W.E., Jenkins M.A., Gould J., Cheney P. (2007) A physics-based approach to modelling grassland fires. *International Journal of Wildland Fire* **16**, 1-22.
- Mell W.E., Maranghides A., McDermott R., Manzello S. (2009) Numerical simulation and experiments of burning Douglas fir trees. *Combustion and Flame* **156**, 2023-2041.
- Parker W.J. (1982) Calculations of the heat release rate by oxygen consumption for various applications, NBSIR 81-2427-1.
- Pope S.B. (2004) Ten questions concerning the large-eddy simulation of turbulent flows. *New Journal of Physics*, **6**, 1-24.
- Porterie B., Consalvi J.L., Kaiss A., Loraud J.C. (2005) Predicting wildland fire behaviour and emissions using a fine-scale physical model. *Numerical Heat Transfer, Part A* **47**, 571-591.
- Quintiere J.G. (2006) *Fundamentals of Fire Phenomena*. (Eds John Wiley & Sons Ltd, The Atrium, Southern Gate, Chichester, England)
- Santoni P.A., Morandini F., Barboni T. (2011) Determination of fireline intensity by oxygen consumption calorimetry. *Journal of Thermal Analysis and Calorimetry*, **104(3)**, 1005-1015,
- Tihay V., Morandini F., Santoni P.A., Pere-Ramirez Y., Barboni T. (2012) Study of the influence of fuel load and slope on a fire spreading across a bed of pine needles by using oxygen consumption calorimetry. *Journal of Physics: Conference Series*, **395**, 012075
- Viegas D.X. (2004) On the existence of a steady state regime for slope and wind driven fires. *International Journal of Wildland Fire*, **13**, 101-117